

Imaging in Gestational Trophoblastic Disease



Lawrence Hsu Lin, MD, PhD,* Rodrigo Polizio, MD,† Koji Fushida, MD, PhD,* and Rossana Pulcineli Vieira Francisco, MD, PhD*

Gestational trophoblastic disease (GTD) is a spectrum of disorders characterized by abnormal trophoblastic proliferation. GTD includes benign conditions such as hydatidiform moles and malignant diseases that are referred as gestational trophoblastic neoplasia (GTN). Ultrasound plays a central role in the diagnosis of patients with hydatidiform mole. Other imaging modalities are useful in molar pregnancy, mainly for evaluating pulmonary complications and atypical presentation of hydatidiform mole. GTN typically arises after 20% of molar pregnancies but can uncommonly occur after nonmolar gestations. After uterine evacuation, serial human chorionic gonadotropin levels are evaluated in patients for early detection of GTN. Once GTN is suspected, Doppler ultrasound is the primary tool to confirm the diagnosis; however, magnetic resonance imaging can also help in selected cases. Metastatic disease workup can involve various modalities, including ultrasound, X-ray, computed tomography, magnetic resonance imaging and positron emission tomography/computed tomography. In this article, we review the main imaging modalities used to evaluate patients with GTD.

Semin Ultrasound CT MRI 40:332-349 © 2019 Elsevier Inc. All rights reserved.

Introduction

Gestational trophoblastic disease (GTD) is a group of conditions that are characterized by the abnormal proliferation of placental trophoblasts. The most common form is hydatidiform mole, which is a benign condition that progresses to malignant forms in up to 20% of cases.¹⁻³ Gestational trophoblastic neoplasia (GTN) represents the malignant counterparts of GTD and comprises invasive mole, choriocarcinoma, placental site trophoblastic tumor (PSTT) and epithelioid trophoblastic tumor (ETT).^{4,5} Imaging plays a central role in the diagnosis of hydatidiform mole and GTN along with clinical findings and human chorionic gonadotropin (hCG) levels.^{6,7} In this article, we review the main imaging modalities used to evaluate patients with GTD.

Hydatidiform Mole

Hydatidiform mole is the most common form of GTD and has an estimated frequency of 1:1000 pregnancies in North America and Europe but is estimated to be even more common in South America and Asia.^{3,8} Hydatidiform mole is classified into 2 entities due to different histologic, genetic, and clinical characteristics: complete hydatidiform mole (CHM) and partial hydatidiform mole (PHM).^{2,9} The major imaging technique used to evaluate hydatidiform mole is ultrasound. With the advancement in ultrasound technology, hydatidiform moles are being diagnosed earlier, and their sonographic presentation is dependent on gestational age.^{10,11} Magnetic resonance imaging (MRI) plays a role in evaluating hydatidiform moles with atypical presentations.¹²⁻¹⁴

Although hydatidiform moles are being diagnosed earlier worldwide, in developing countries, there are still patients diagnosed after the first trimester, leading to the development of complications associated with molar pregnancy.¹⁵ Chest X-ray (CXR) and computed tomography (CT) scans can be used to evaluate pulmonary complications of hydatidiform moles, especially when patients present with acute respiratory distress.^{16,17}

Complete Hydatidiform Mole

CHM is a diploid androgenetic pregnancy characterized by abnormal proliferation of trophoblastic tissue without

*University of Sao Paulo Trophoblastic Disease Center, Department of Obstetrics and Gynecology, University of Sao Paulo Medical School, Sao Paulo, Brazil.

†Sao Paulo State Cancer Center, Department of Oncology and Radiology, University of Sao Paulo Medical School, Sao Paulo, Brazil.

Address reprint requests to Lawrence Hsu Lin, MD, PhD, Department of Obstetrics and Gynecology, University of Sao Paulo Medical School, Av. Dr. Eneas de Carvalho Aguiar 255, 10th Floor, Sao Paulo 05403-000 Brazil. E-mail: l.lin@hc.fm.usp.br

evidence of embryonic development.^{2,18} The presentation of CHM on ultrasound depends on gestational age; therefore, the rate of ultrasound detection of CHM increases with gestational age.^{19,20} Early CHM can mimic sonographic images of an embryonic death (Fig. 1a), an incipient pregnancy (Fig. 2a), or a blighted ovum (Fig. 3a); however, with increased gestational age, these molar pregnancies take on a classical sonographic appearance for CHM.^{20,21} The typical sonographic features of heterogeneous intrauterine material with multiple cysts typically arise at the end of the first trimester (Fig. 1b, 2b, 3b). Hydropic abortions can raise the suspicion of a hydatidiform mole when there is intense villosus swelling (Fig. 4a). The differential diagnosis can be made with hCG measurements before uterine evacuation or with histopathologic analysis after this procedure.^{19,21-23} In patients with hydatidiform moles and high levels of hCG,

theca-lutein cysts can be found in the adnexa (Fig. 5a-c), which regress months after uterine evacuation without additional treatment.²⁴

Partial Hydatidiform Mole

PHM is a triploid androgenetic pregnancy composed of an enlarged placenta and abnormal fetus.^{9,18} Similar to CHM, the sonographic presentation of PHM is dependent on gestational age.¹⁹ Early sonographic diagnosis of PHM is more difficult than that of CHM because of the presence of a conceptus that can mimic a normal early pregnancy (Figs. 6a and 7a); therefore, PHM is typically suspected later in the first trimester when a thickened placenta is visible (Figs. 6b and 7b).²⁵ Intrauterine growth retardation,

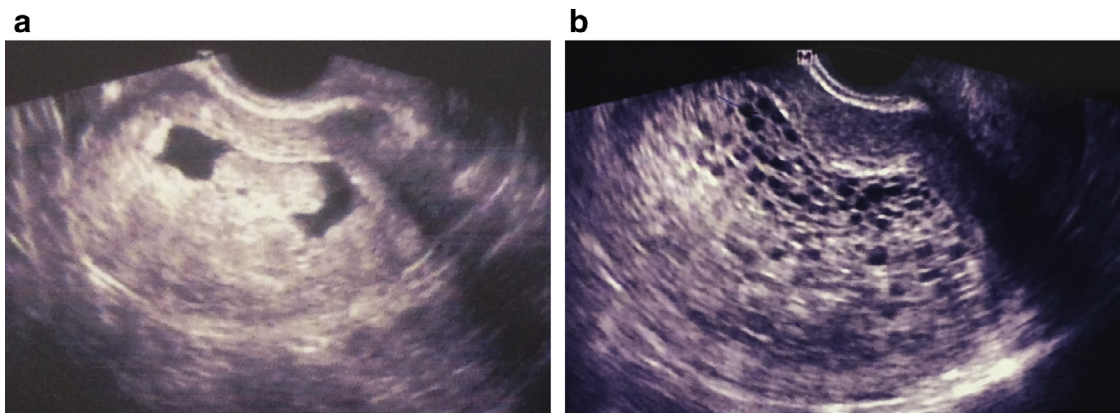


Figure 1 Complete hydatidiform mole. (a) Transvaginal grayscale ultrasound image showing a hyperechogenic area with no cardiac activity inside an irregular intrauterine gestational sac at 7 weeks' gestation. (b) Transvaginal grayscale ultrasound image showing a classical CHM appearance characterized by a heterogeneous intrauterine mass with multiple small round anechoic structures at 11 weeks' gestation after expectant management based on an initial diagnosis of embryonic death.

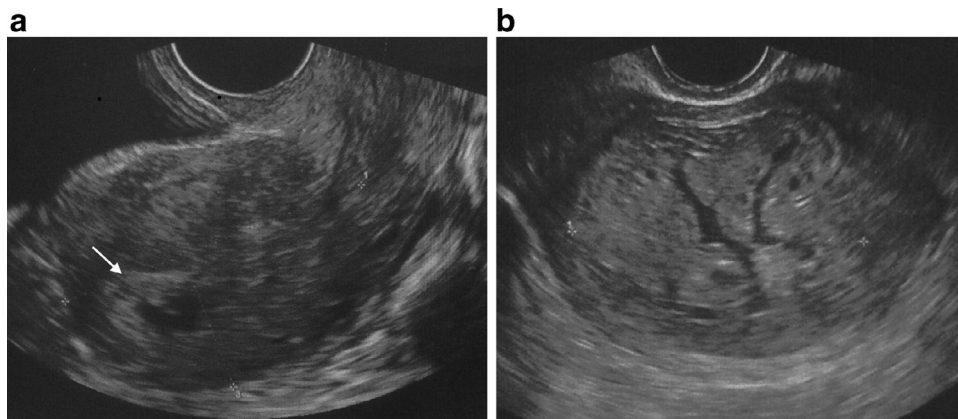


Figure 2 Complete hydatidiform mole. (a) Transvaginal grayscale ultrasound image showing a small irregular gestational sac with no embryo inside at 9 weeks' gestation. (b) Transvaginal grayscale ultrasound image showing a large heterogeneous intrauterine mass with a few cysts at 12 weeks' gestation after expectant management based on an initial diagnosis of incipient pregnancy.

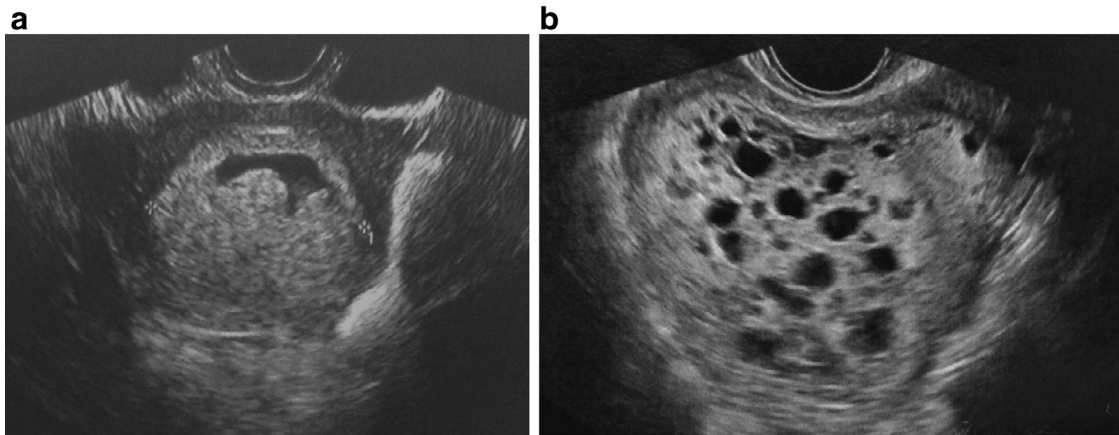


Figure 3 Complete hydatidiform mole. (a) Transvaginal grayscale ultrasound image showing an irregular gestational sac with a thickened placental area and no embryo at 8 weeks' gestation. (b) Transvaginal grayscale ultrasound image showing classic sonographic features of CHM with a heterogeneous intrauterine mass with multiple round anechoic structures at 11 weeks gestation after expectant management based on an initial hypothesis of a blighted ovum.

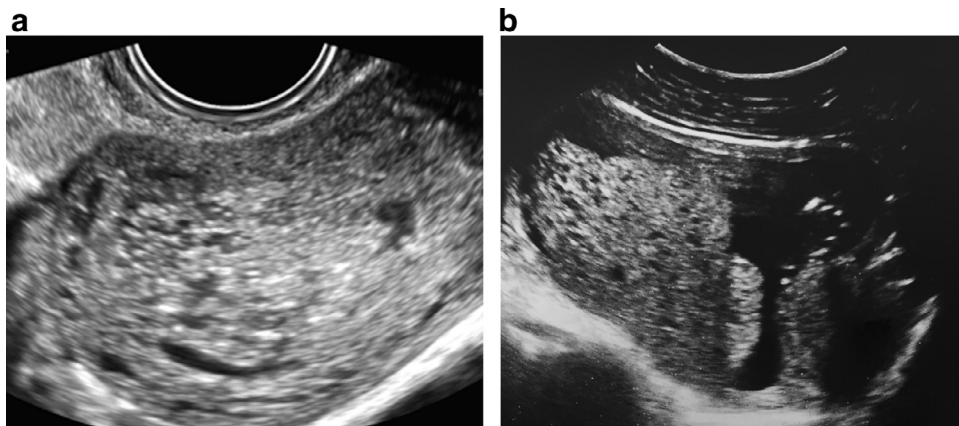


Figure 4 Nonmolar hydropic abortion. (a) Transvaginal grayscale ultrasound images showing a heterogeneous intrauterine mass with cystic areas. (b) Transvaginal grayscale ultrasound image showing a thickened placenta with cystic changes and a hydropic fetus secondary to severe fetal anemia.

fetal structural abnormalities, and placental cystic changes are usually observed during the second trimester (Fig. 7c and d).²⁶ Hydropic abortion can also mimic PHM, especially when there is a visible embryo (Fig. 4b), making hCG levels an important tool to establish the diagnosis.^{19,21,23} Antenatal invasive procedures involving cytogenetic analysis can also aid in the diagnosis and often reveal triploidy. During the first trimester, PHM is usually diagnosed on histopathologic analysis.^{21,22,25} Theca-lutein cysts can also be present when hCG levels are high (Fig. 5a-c).²⁴

Multiple Pregnancies with Complete Mole and a Normal Coexisting Fetus

Multiple pregnancies with complete mole and a normal coexisting fetus is a rare condition that is a differential

diagnosis for partial mole due to the presence of a fetus. The estimated incidence of this condition is 1:20,000-100,000 pregnancies.^{27,28} Ultrasound is the initial tool used to evaluate these pregnancies, and two distinct placental images are visible: one with molar changes and the other with a normal appearance associated with a fetus with no structural abnormalities (Fig. 8a-e). Sonographic diagnosis is not always able to confirm this diagnosis; therefore, MRI can be used as an ancillary tool that helps to differentiate the two different placental areas and determine the interface with the myometrium (Fig. 9a and b).^{12,13} Differential diagnoses include PHM, placental mesenchymal dysplasia, and other causes of hydropic placentas (eg, fetal anemia). Cytogenetic analysis from amniocentesis or chorionic villous sampling can also help in determining the prenatal diagnosis.²⁷

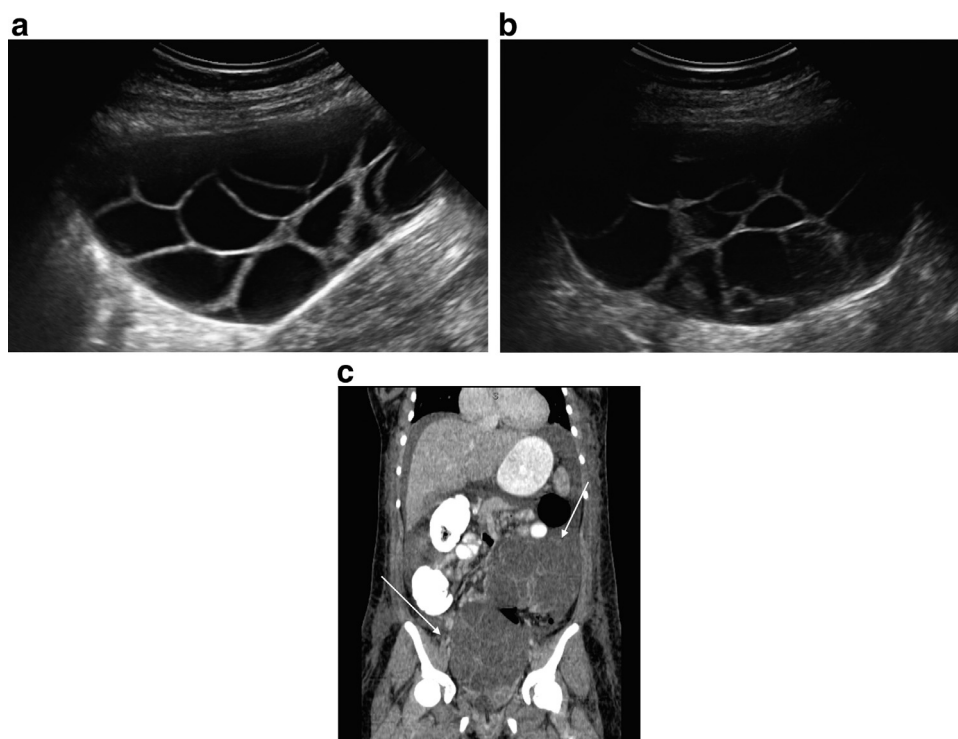


Figure 5 Theca-lutein cysts. (a,b) Transabdominal grayscale ultrasound image showing an enlarged ovary with multiple large anechoic cysts. (c) Coronal CT image showing numerous theca-lutein cysts on both ovaries (solid arrow).

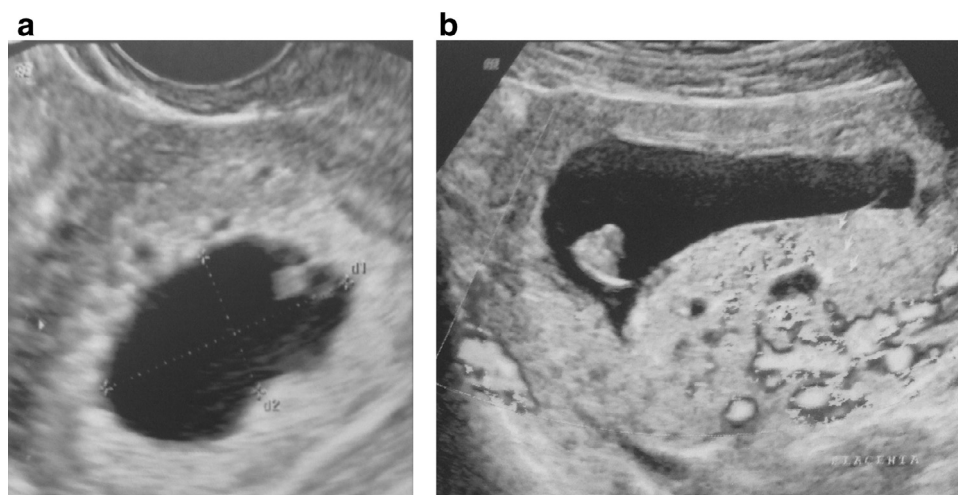


Figure 6 Partial hydatidiform mole. (a) Transvaginal grayscale ultrasound image showing a gestational sac with an embryo and yolk sac at 6 weeks' gestation. (b) Follow-up transabdominal grayscale ultrasound image showing embryonic death and a thickened placenta with cystic changes at 10 weeks' gestation.

Ectopic Molar Pregnancies

Hydatidiform moles can also arise outside the uterine cavity, similar to nonmolar pregnancies. There have been cases reported in the literature of hydatidiform moles in the fallopian tube, ovary, and cesarean section scar, and heterotopic pregnancies.²⁹⁻³¹ The initial imaging tool used to evaluate

ectopic hydatidiform moles is usually ultrasound, and most cases do not exhibit typical features of intrauterine molar pregnancies; therefore, pre-evacuation diagnosis is suspected due to high levels of hCG.³² MRI can aid the diagnosis and treatment planning for hydatidiform moles in unusual locations (eg, cesarean scar hydatidiform mole)³³ (Fig. 10a-c).

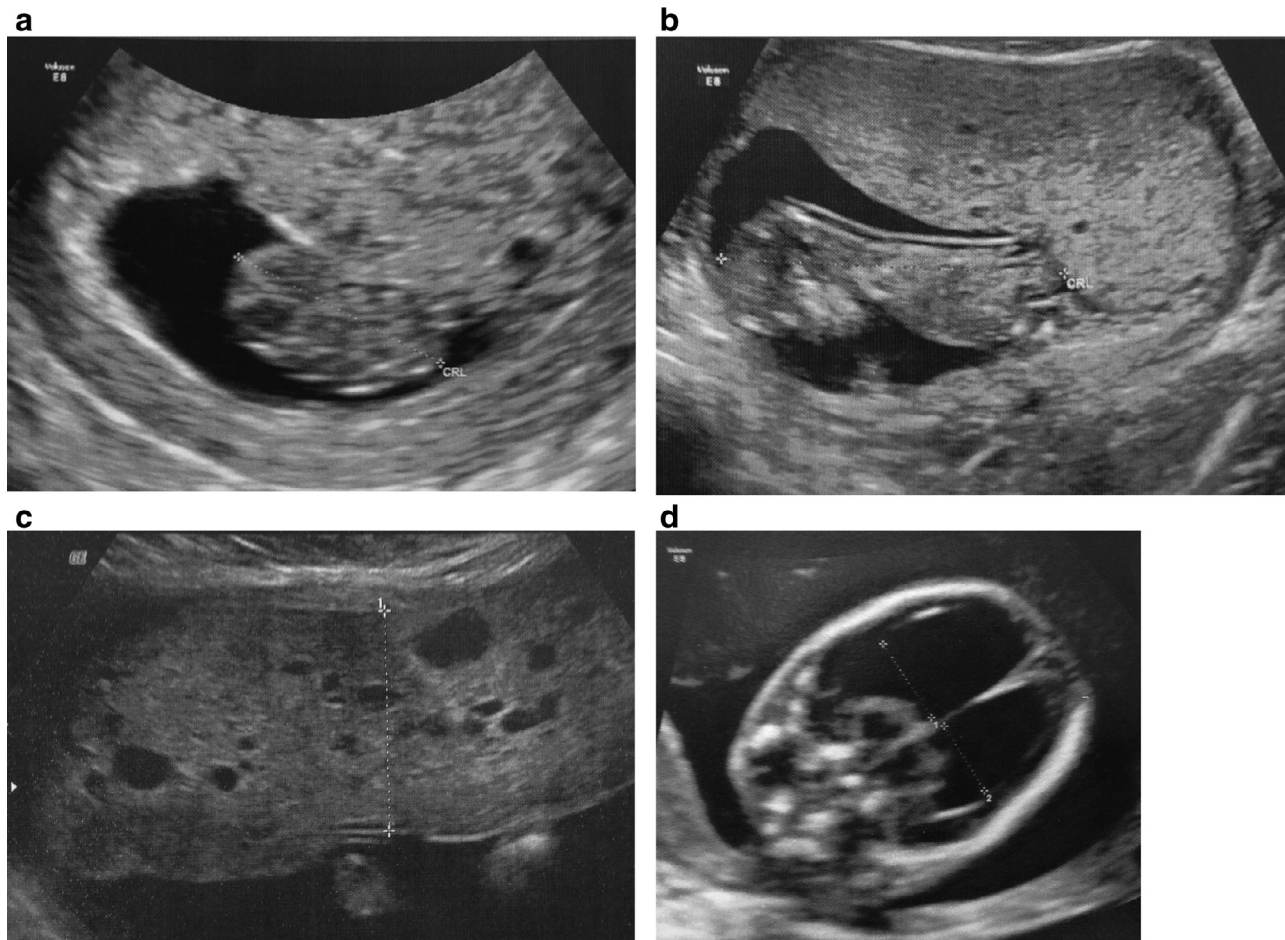


Figure 7 Partial hydatidiform mole. (a) Transvaginal grayscale ultrasound image showing a gestational sac with an embryo at 9 weeks' gestation. (b) Transabdominal grayscale ultrasound image showing a fetus with no morphologic anomalies and a thickened placenta with subtle cystic changes at 13 weeks' gestation. (c) Transabdominal grayscale ultrasound image showing a thickened placenta with remarkable cystic changes at 18 weeks' gestation. (d) Transabdominal grayscale ultrasound image showing an axial cross-section of a fetal head with severe bilateral ventriculomegaly at 18 weeks' gestation.

Uterine Evacuation of Molar Pregnancies

Uterine evacuation of molar pregnancies at advanced gestational age can be challenging due to the large uterine volume; therefore, the risks of bleeding, perforation, and incomplete evacuation are increased.³⁴ Intraoperative ultrasound performed abdominally can aid during the procedure, lowering the risk of complications (Fig. 11).

Pulmonary Complications of Hydatidiform Moles

Patients with molar pregnancies in advanced gestational age can present with clinical complications. The most common complications include the following: vaginal hemorrhage, preeclampsia, hyperemesis, and hyperthyroidism.¹⁰ Pulmonary complications are less common; however, they can be life-threatening, and patients should be promptly evaluated and treated. There are several causes of respiratory failure in patients with hydatidiform mole, including pulmonary edema, pleural effusion, pulmonary embolism, and trophoblastic

embolization.^{16,35} The radiographic features of pulmonary edema, pleural effusion, and pulmonary embolism in patients with molar pregnancies do not differ from those in patients without this condition.

Trophoblastic embolization is a potentially life-threatening condition that specifically affects patients with late hydatidiform moles and often occurs during uterine evacuation or after the use of uterotonic drugs.³⁶ This complication is characterized by a massive migration of trophoblastic cells to the pulmonary vessels, causing acute respiratory failure. In severe cases, CXRs typically show bilateral diffuse pulmonary infiltrates (Fig. 12a). Chest CT is the modality of choice for the diagnosis of trophoblastic embolization with findings that resemble those of acute respiratory distress from other causes (Fig. 12b and c), including widespread areas of increased attenuation, such as ground-glass opacities and consolidation. Findings secondary to pulmonary edema, such as pleural effusion and thickening of septal lines, can also be seen because these patients tend to receive large amounts of fluids. Because the migration of trophoblastic cells occurs via small capillaries,

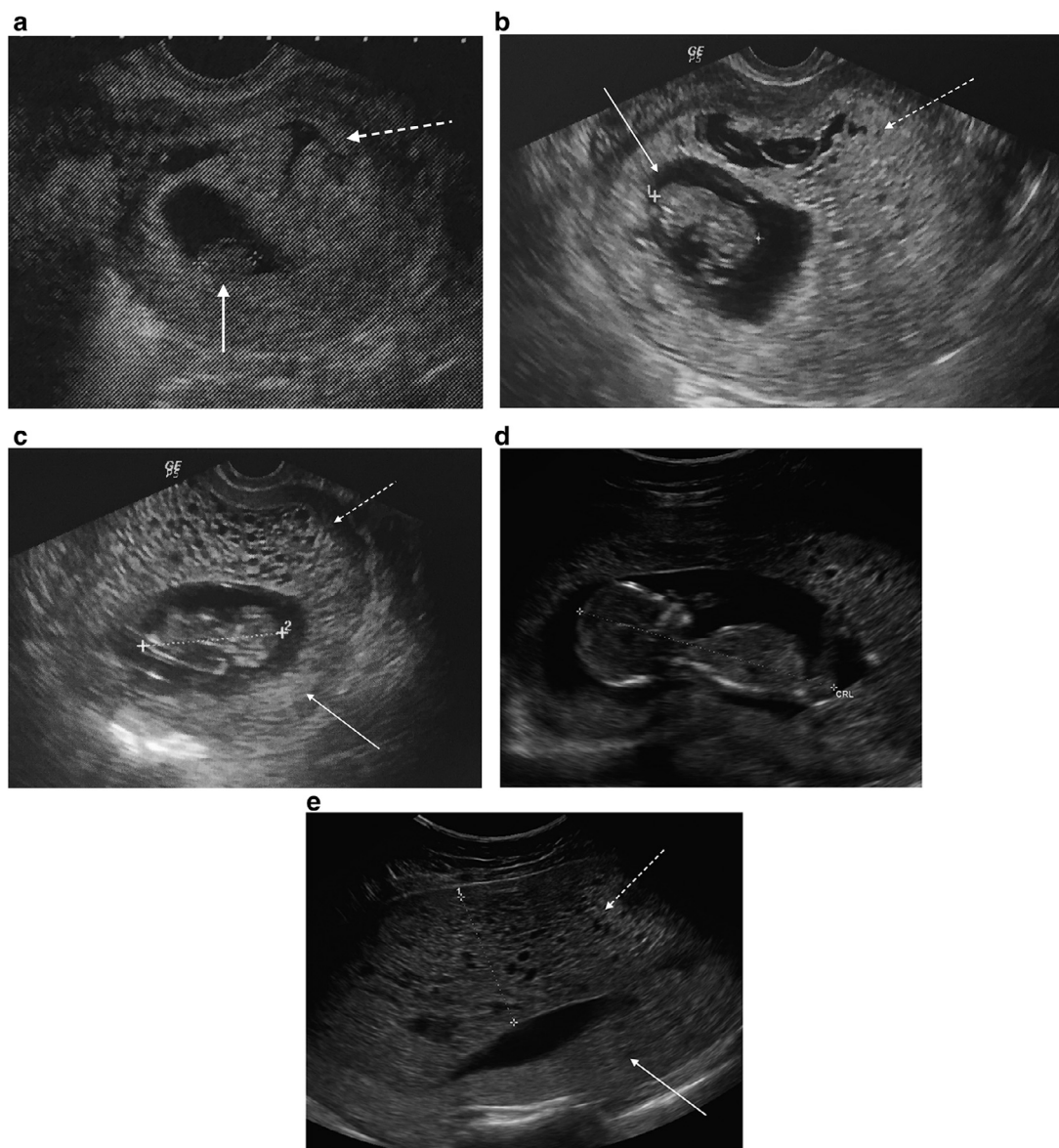


Figure 8 Twin pregnancy with complete mole and a normal coexisting fetus. (a) Transvaginal grayscale ultrasound image showing two gestational sacs, one with an embryo (solid arrow) and another with a heterogeneous mass inside (dashed arrow), at 7 weeks' gestation. (b) Transvaginal grayscale ultrasound image showing two gestational sacs, one with an embryo (solid arrow) and another with a heterogeneous mass with subtle cystic changes (dashed arrow), at 8 weeks' gestation. (c) Transvaginal grayscale ultrasound image showing an embryo with two placental masses: a thickened placenta with multiple cysts (dashed arrow) and another with no abnormalities (solid arrow) at 11 weeks' gestation. (d) Transabdominal grayscale ultrasound image showing a fetus with no structural abnormalities at 15 weeks' gestation. (e) Transabdominal grayscale ultrasound image at 15 weeks' gestation showing a thickened placenta with multiple cysts anteriorly (dashed arrow) and another with no abnormalities posteriorly (solid arrow).

no visible emboli of major pulmonary arteries are usually detected.^{16,17,35}

Gestational Trophoblastic Neoplasia

Evaluation of the Primary Tumor

After uterine evacuation, the hCG levels and clinical parameters of patients with a diagnosis of hydatidiform moles are

monitored for early detection of GTN.^{1,3} Ultrasound is the primary method and should be used to evaluate patients with increased or plateaued hCG levels, not only to diagnose possible GTN but also to exclude the possibility of a new pregnancy before the initiation of treatment. GTN patients who receive proper therapy usually have a good prognosis, even in the presence of metastasis; therefore, recognition and prompt treatment are fundamental.^{1,3,5}

There are no typical sonographic and Doppler characteristics of GTN; therefore, correlation with hCG levels is vital to establish a differential diagnosis with other conditions that

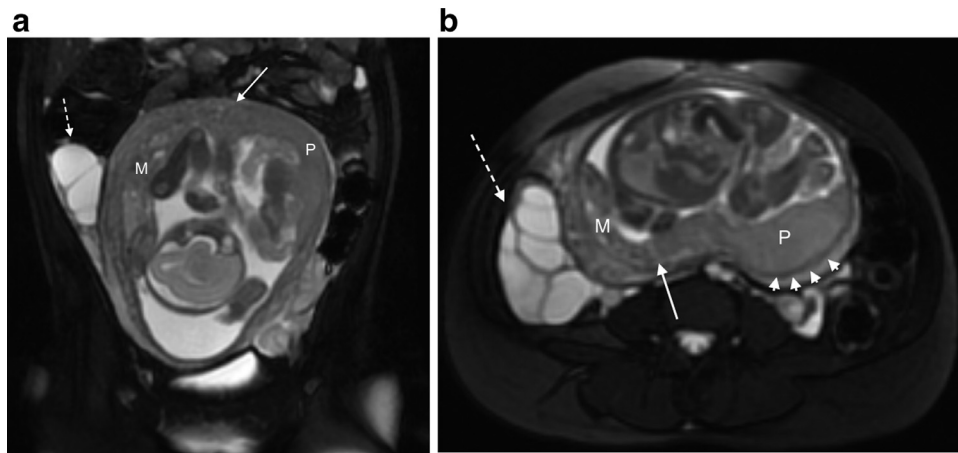


Figure 9 Coronal (a) and axial (b) balanced steady-state free precession (FIESTA) image showing a normal fetus in the uterine cavity with a normal placental insertion at the left fundus (letter P) and a complete mole at the right uterine fundus (letter M) characterized by a heterogeneous and elongated mass with small cystic formations. A fine line with a low signal that separates the normal placenta and the complete mole (solid arrow) and another fine line with a low signal that separates the mole and the placenta from the inner myometrium (arrowheads) are present. Right ovary with enlarged dimensions and multiple theca-lutein cysts (dashed arrow).

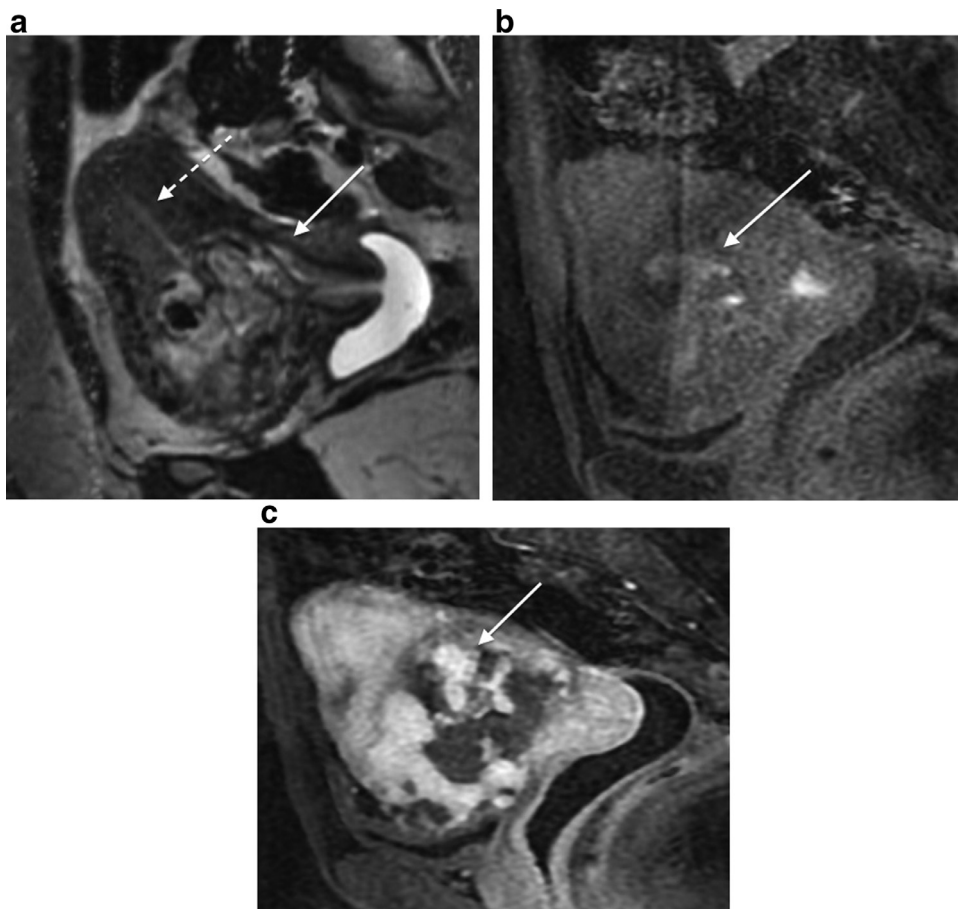


Figure 10 (a) Reformatted sagittal T2-weighted MRI showing a uterine mass (solid arrow) at the cervical/isthmus transition (C-section scar topography) with an empty uterine cavity (dashed arrow). The mass is heterogeneous with some cystic spaces. (b) Sagittal fat-suppressed T1-weighted image showing hemorrhagic foci on the mass. (c) Sagittal gadolinium-enhanced fat-suppressed T1-weighted image showing heterogeneous enhancement of the solid components of the mass.

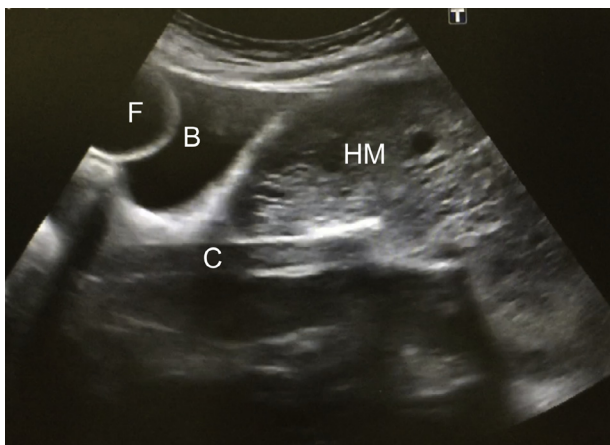


Figure 11 Transabdominal grayscale ultrasound image showing an ultrasound-guided uterine evacuation of a complete mole. Bladder (B), Foley catheter (F), evacuation canula (C), hydatidiform mole (HM).

can mimic a GTN, such as fibroids, retained products of conception, pelvic inflammatory disease, arteriovenous malformations, or other uterine malignancies.³⁷⁻³⁹

Sonographic imaging in GTN can present with a variety of different features. A hyperechogenic, hypoechogenic or heterogeneous myometrial mass can be found, and there is often no clear interface with the endometrium (Fig. 13a-c). In some cases, the presence of cystic areas in the myometrium resembles an invading hydatidiform mole (Fig. 13c). However, there are no sonographic characteristics that can clearly differentiate between the histologic types of GTN.^{6,38} Therefore, patients with a sonographic image suggestive of GTN and low levels of hCG should raise the suspicion of a PSTT/ETT, since these intermediate trophoblast tumors produce only small amounts of hCG.^{40,41}

Doppler ultrasound can aid in the evaluation of GTN since it is a group of highly vascularized tumors.^{38,39} Hsieh et al described 3 different vascular patterns of GTN: diffuse, lacunar, and compact. The diffuse pattern is characterized by a nonspecific myometrial vascularization (Fig. 14a); the lacunar pattern involves by vascular lacunae within a complex myometrial mass with a turbulent flow (Fig. 14b); and the compact pattern is observed in patient with a hyperechogenic mass with peripheral low-resistance vascularization with an avascular central area⁴² (Fig. 14c).

Uterine artery Doppler velocimetry before the initiation of chemotherapy has been shown to be correlated with GTN resistance to methotrexate. A pulsatility index of less than 1.0 seems to be a risk factor for methotrexate resistance in low-risk GTN.^{43,44} There is also evidence that lower uterine artery Doppler velocimetry indices before and after surgical evacuation of hydatidiform mole are predictive of GTN.⁴⁵

CT is used mainly for the evaluation of distant metastasis, because, the use of this modality in the assessment of uterine disease is limited. GTN typically presents as a low-attenuation uterine mass on CT with local enhancement after administration of contrast (Fig. 15a and b).

On MRI, GTN presents as an isointense (on T1-weighted images) and hyperintense (on T2-weighted images) irregular uterine mass that distorts the junction zone with intense signal enhancement of the lesion after the administration of gadolinium (Fig. 16a-c). Because GTN lesions are highly vascularized tumors, numerous vessels can be seen within the myometrium and surrounding the uterus.^{6,7,46}

MRI is not usually needed in the routine evaluation of GTN. However, this imaging modality can be useful in patients with atypical presentation (Figs. 17a-d and 18a-d), recurrence (Fig. 19), and PSTT/ETT (Figs. 20a-d and 21).^{32,41,46} Similar to the ultrasound appearance of GTN, there are no features on MRI that are specific to GTN, and

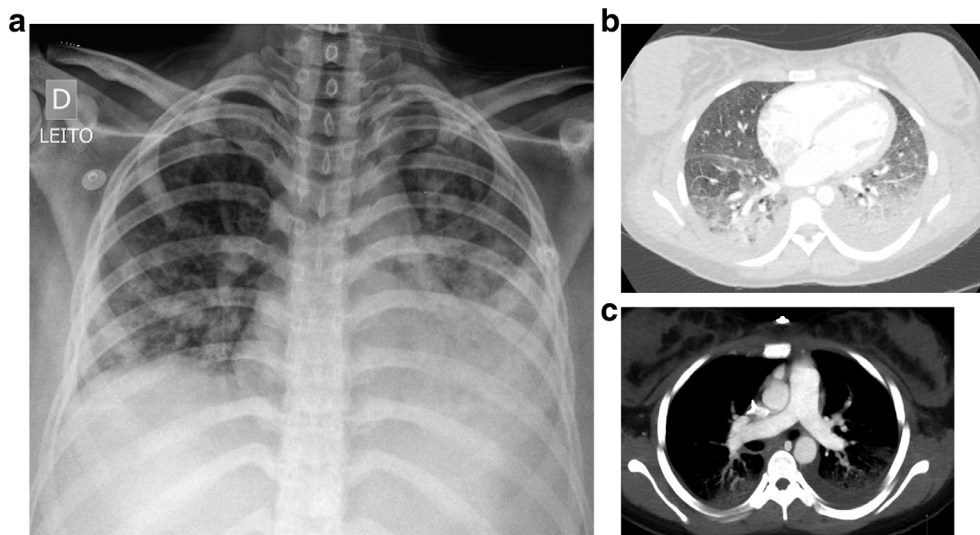


Figure 12 Trophoblastic embolization. (a) Anteroposterior CXR showing diffuse pulmonary infiltrates. (b) Axial CT image with a lung window showing widespread patchy ground-glass opacities and consolidations. (c) Axial contrast-enhanced CT image showing bilateral pleural effusion and no signs of arterial embolism of the major pulmonary arteries.

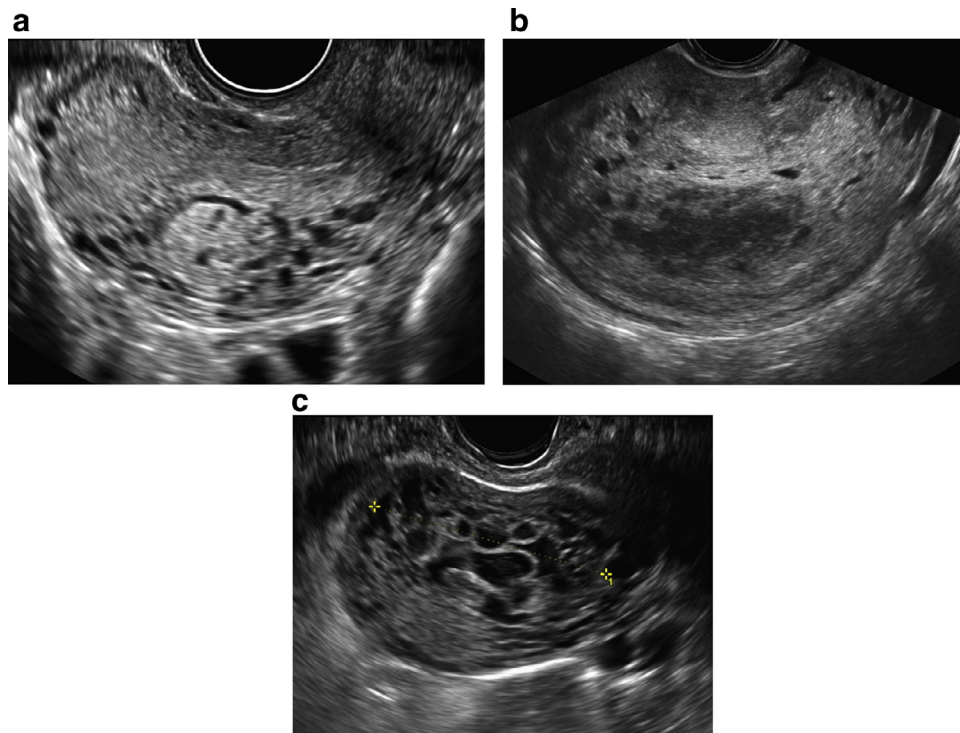


Figure 13 Gestational trophoblastic neoplasia. (a) Transvaginal grayscale ultrasound image showing a sagittal section of the uterus with a myometrial hyperechogenic mass invading the posterior uterine wall and round anechoic structures corresponding to vessels surrounding the tumor in a patient with increased hCG levels after the evacuation of a hydatidiform mole. (b) Transvaginal grayscale ultrasound image showing a sagittal section of the uterus with a large heterogeneous mass with hyperechogenic and hypoechogenic with no clear interface between the endometrium and myometrium in a patient with increased hCG levels during the postmolar follow-up. (c) Transvaginal grayscale ultrasound image showing an axial section of the uterus with multiple cysts separated by a thin septum in the anterior wall resembling a hydatidiform mole invading the myometrium in a patient with increased hCG levels after uterine evacuation of a hydatidiform mole.

there are no characteristics that are able to distinguish between GTN types; therefore, clinical information and laboratory tests are essential for the diagnosis of GTN.

MRI is also helpful for evaluating the primary tumor and local disease invasion in patients who are undergoing surgical treatment, since this modality is superior to ultrasound and CT for the assessment of parametrium, vagina, and pelvic lymph nodes.

Evaluation of Metastatic Disease

After the diagnosis of GTN, it is important to stage and screen for the presence of metastasis. The International Federation of Gynecologists and Obstetricians (FIGO) suggests the use of 2 different staging systems: anatomical and prognostic factor staging.³ Anatomical staging is based only on the location of the malignant disease and metastasis (Table 1) and does not help in determining treatment. The FIGO/World Health Organization (WHO) (2000) prognostic factor staging includes multiple risk factors and is better correlated with prognosis and treatment outcomes than anatomical staging (Table 2). Patients who score 6 or less on the FIGO/WHO prognostic factor staging system are classified as low

risk, while those who score 7 or more are categorized as high risk. Patients with multiple risk factors with a score of 12 or more fall into a particular group called ultra-high risk.³

The most common site of metastatic GTN is the lung, followed by vagina, liver, and brain. Other sites have also been reported, such as the bowels, spleen, kidneys, and bones. Initial screening for metastasis includes clinical examination for genital metastasis and chest CXR.⁴⁷ If CXR and physical examination findings are normal, no further evaluation is needed in typical cases of GTN and treatment can be started. If CXR findings are normal, chest CT is not usually needed, since this modality detects micrometastases, which do not change the prognosis of patients and can be present in up to 40% of patients.^{48,49} In the presence of very high hCG levels, GTN after nonmolar pregnancy or suspicion of ETT or PSTT, it is advisable to perform a complete workup with chest CT, brain MRI, and abdominopelvic MRI or CT.^{41,47,50-52}

Lung metastases are usually visible on CXR when they are larger than 1 cm and present as multiple, well-defined, dense and rounded opacities (Fig. 22a). Chest CT can provide a more detailed evaluation, even though there seems to be no additional prognostic benefit, while CXRs are the initial method used to evaluate lung metastasis.⁴⁷⁻⁴⁹ On chest CT,

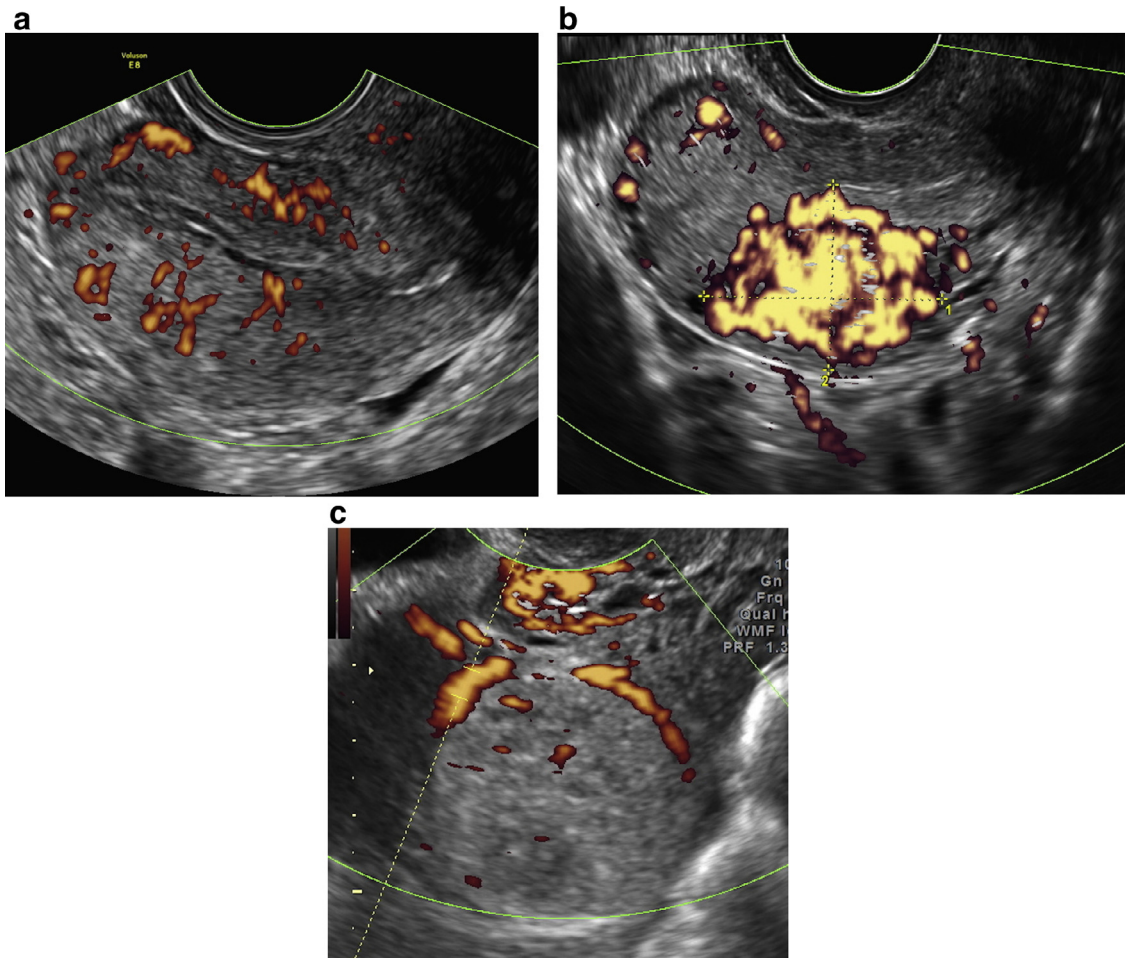


Figure 14 Uterine gestational trophoblastic neoplasia. (a) Transvaginal power Doppler ultrasound image showing a sagittal cross section of the uterus with diffuse increased vascularity in a patient with increased hCG levels after the evacuation of a hydatidiform mole. (b) Transvaginal power Doppler ultrasound image showing a sagittal cross section of the uterus with a highly vascularized mass with blood lacunae in a patient with increased hCG levels during postmolar follow-up. (c) Transvaginal power Doppler ultrasound image showing a hyperechogenic round mass with low-resistance peripheral vascularity in a patient with very high hCG levels after the evacuation of a complete mole. Histologic analysis revealed a choriocarcinoma.

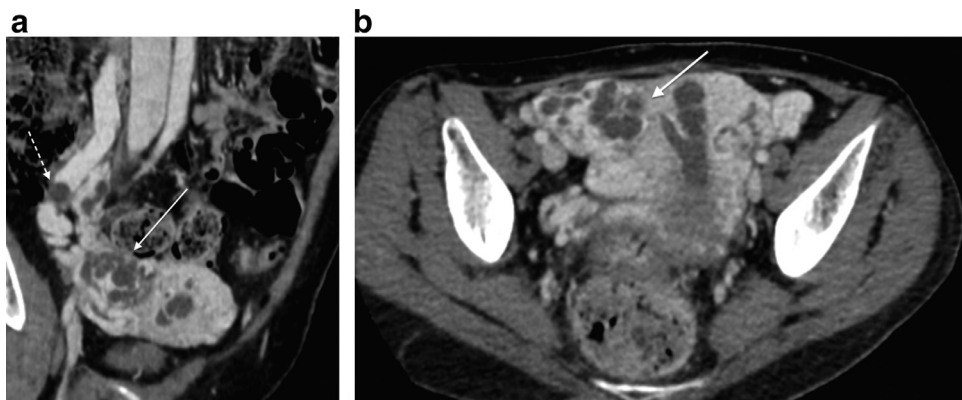


Figure 15 Uterine gestational trophoblastic neoplasia. (a) Reformatted coronal and (b) contrast-enhanced CT images showing a uterine mass with extraterine dissemination in the right adnexal region (solid arrow). The mass is heterogeneous and highly vascularized with enhancement by the contrast media and is surrounded by numerous and tortuous engorged vessels. Note the ovarian right vein with an enlarged caliber with an endoluminal thrombus (dashed arrow).

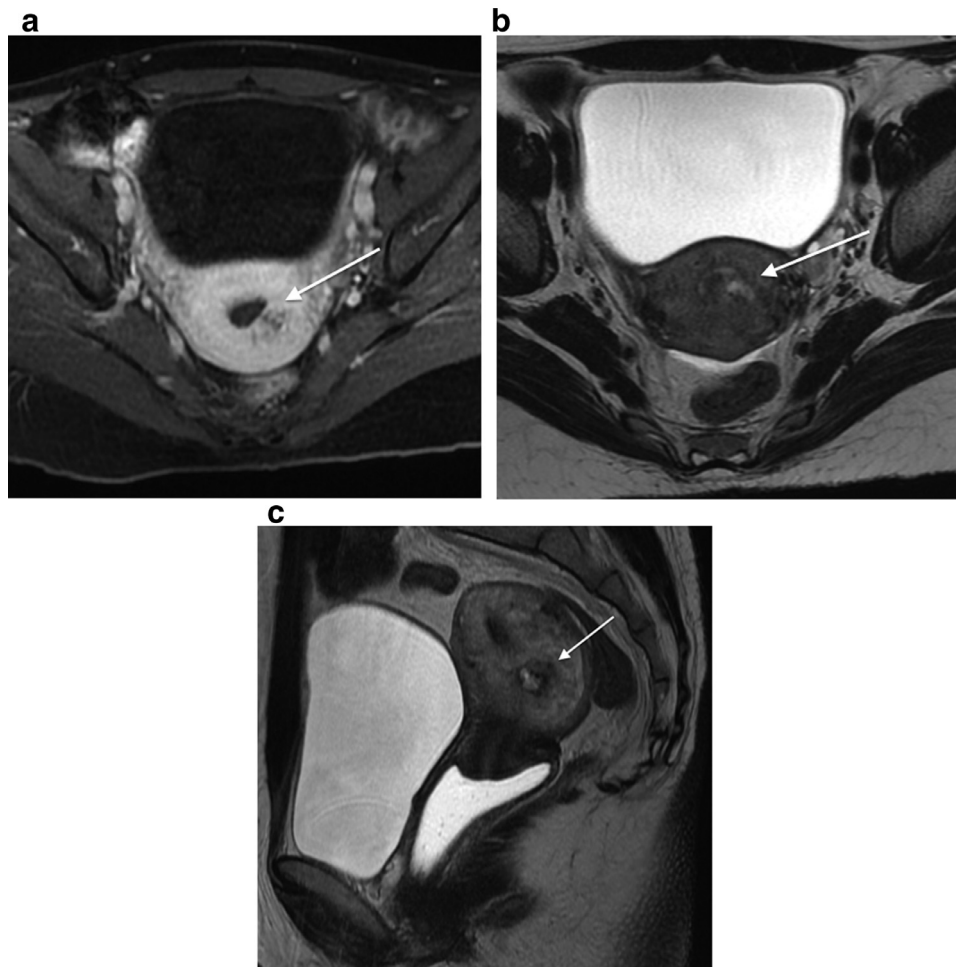


Figure 16 Uterine gestational trophoblastic neoplasia. (a) Axial and (b) sagittal T2-weighted images showing a heterogeneous mass with a predominantly high signal centered in the inner myometrium (solid arrow). The interface between the mass and surrounding myometrium is ill defined. (c) Axial gadolinium-enhanced fat-suppressed T1-weighted image showing moderate enhancement of the mass.

pulmonary metastases often present as multiple, rounded, well-defined nodules (Fig. 22b and c). Less commonly, lung metastases can present as single nodules, cavitations, pleural effusion (pleural disease), atelectasis (endobronchial disease), or embolic disease with intravascular tumors or pulmonary infarctions.

Brain and liver metastases are rare and usually arise in patients with nonmolar pregnancies or those with a late diagnosis of GTN; therefore, such metastases represent important risk factors for a poor prognosis.^{53,54}

Liver metastases are usually multiple, heterogenous, rounded, hypodense masses with enhancement in the arterial phase after intravenous contrast administration on CT (Fig. 23a). Similar characteristics are seen on MRI, with hyperintense nodules on T2-weighted images with signal enhancement after gadolinium administration (Fig. 23b).

Brain metastases can be visualized on brain CT (Fig. 24a) but are better evaluated with MRI (Fig. 24b-d). There can be single or multiple heterogenous masses, often located at the gray-white matter interface. Due to the high vascularization of brain metastases, such metastases can lead to spontaneous

intracranial hemorrhage, which is visualized as high attenuation on CT and variable MRI signal intensity depending on the chronicity.

The role of positron emission tomography/CT (PET/CT) is still not well determined in the management of patients with GTN, since the experience with the use of this modality in this group of diseases is limited. PET/CT might be helpful, especially in patients with recurrent disease.^{47,55}

The abnormal images seen in GTN can persist for months after the completion of treatment; therefore, imaging is not routinely performed during follow-up. Imaging evaluation is often needed if there is suspicion of chemoresistance or recurrent disease, usually based on the increase or stabilization in hCG levels.

Arteriovenous Malformation (AVM)

AVMs are vascular structures resulting from the abnormal communication of arteries and veins. AVMs usually arise in

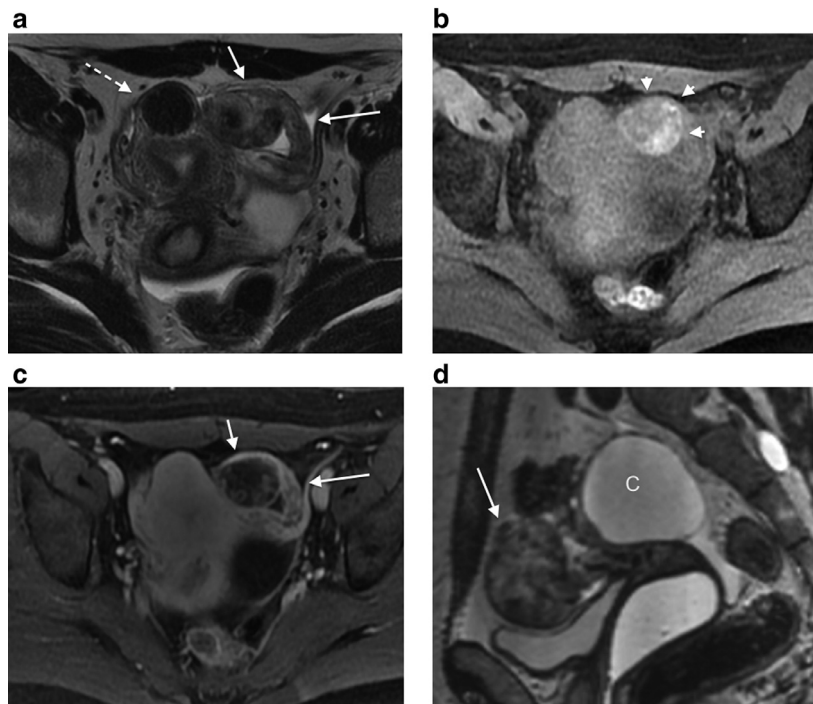


Figure 17 Tubal choriocarcinoma. (a) Axial T2-weighted image showing an enlarged fallopian tube with a mass in the infundibulum with heterogeneous signal intensity (solid arrows). An empty uterine cavity and a fibroid on the uterine fundus are also noted (dashed arrow). (b) Axial fat-suppressed T1-weighted image showing hemorrhagic foci in the mass. (c) Axial gadolinium-enhanced fat-suppressed T1-weighted image showing heterogeneous enhancement of the solid components of the mass (arrowheads). (d) Reformatted sagittal T2-weighted image showing the fallopian tube mass anteriorly (solid arrow) and the left ovary posteriorly with a large simple cyst (letter C).

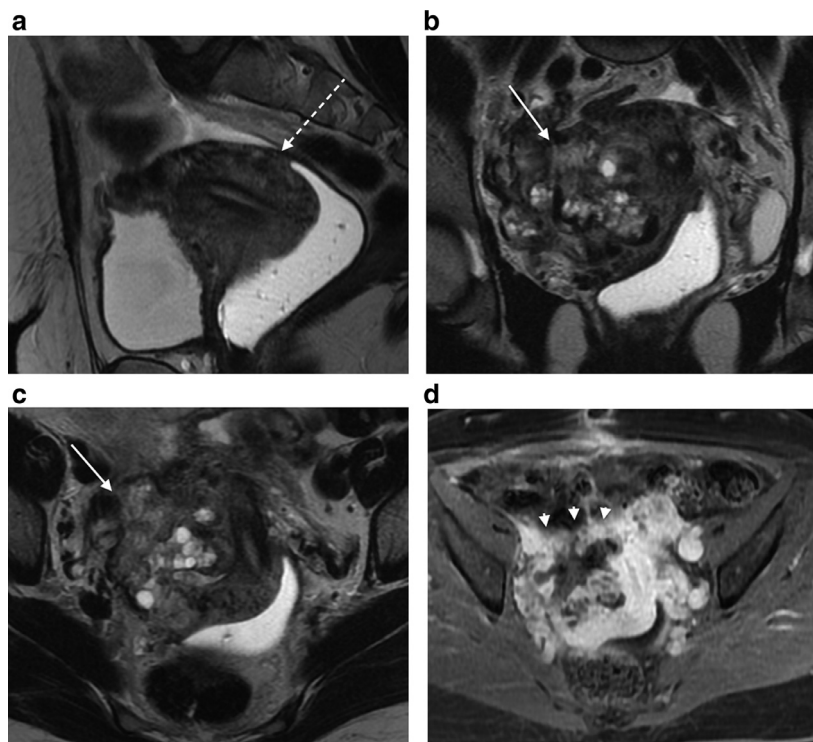


Figure 18 Cervical gestational trophoblastic neoplasia after a subtotal hysterectomy. (a) Sagittal T2-weighted image showing a gel-distended vaginal cavity and signs of subtotal hysterectomy (dashed arrow). (b) Coronal and (c) axial T2-weighted images showing a gel-distended vaginal cavity and a heterogeneous mass in the right paracervical region infiltrating the cervix (solid arrow). (d) Axial gadolinium-enhanced fat-suppressed T1-weighted image showing heterogeneous enhancement of the mass (arrowheads).

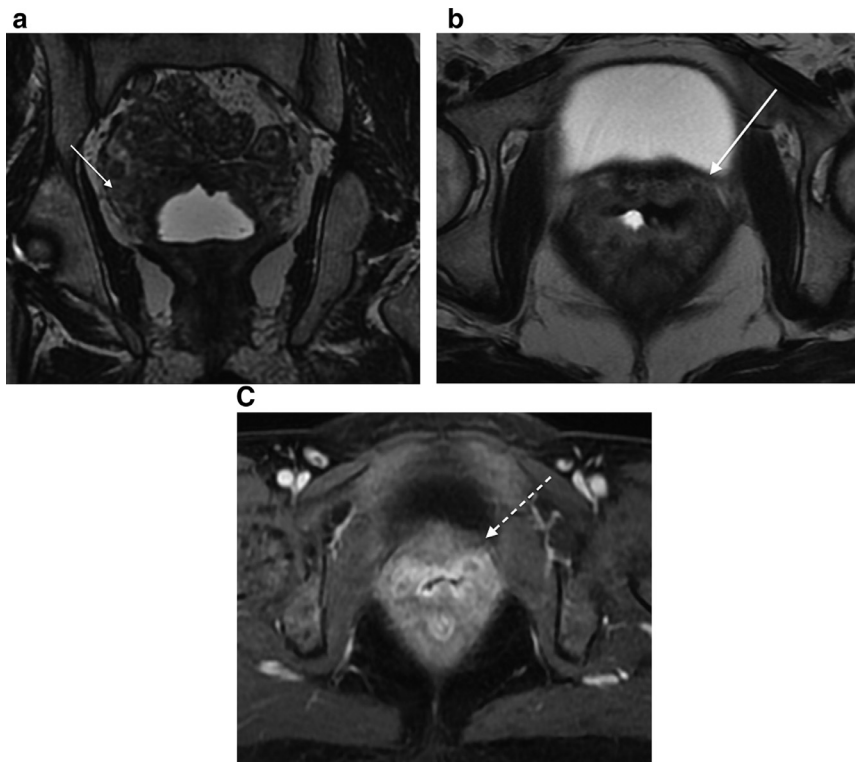


Figure 19 Vaginal cuff recurrent disease after total hysterectomy. (a) Coronal and (b) axial T2-weighted images showing a gel-distended vaginal cavity with heterogeneous thickening of the vaginal walls with nodularity in the adjacent fat tissue (solid arrow) in a patient with increasing levels of hCG. (c) Axial gadolinium-enhanced fat-suppressed T1-weighted image showing heterogeneous enhancement of the vaginal walls (dashed arrow).

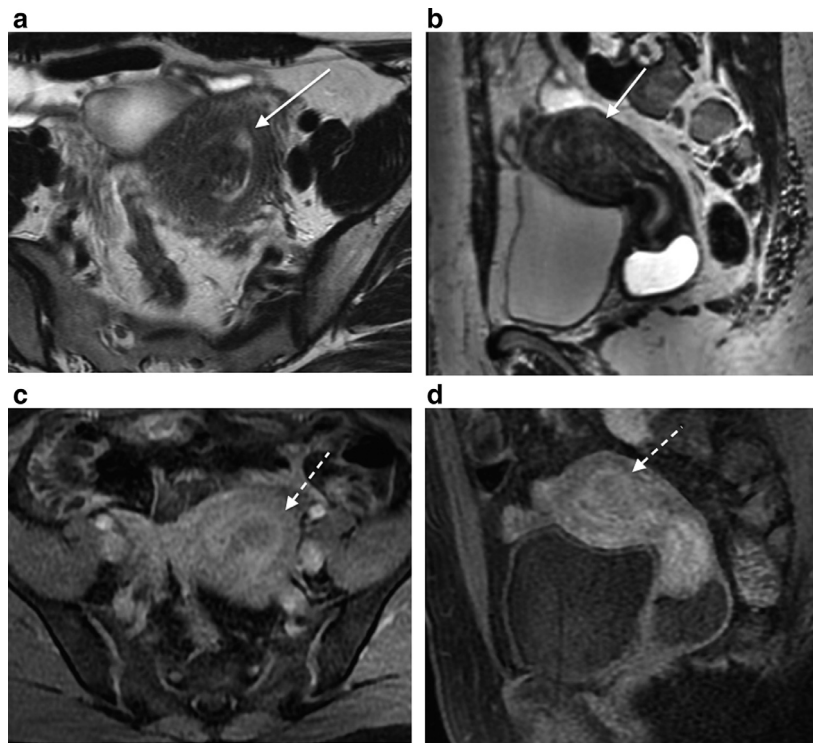


Figure 20 Placental site trophoblastic tumor. (a) Axial and (b) sagittal T2-weighted images showing a heterogeneous mass with a predominantly high signal centered in the inner myometrium distorting the junctional zone and projecting into the uterine cavity (solid arrow). The interface between the mass and surrounding myometrium is ill defined. (c) Axial and (d) sagittal gadolinium-enhanced fat-suppressed T1-weighted images showing moderate enhancement of the mass (dashed arrow).

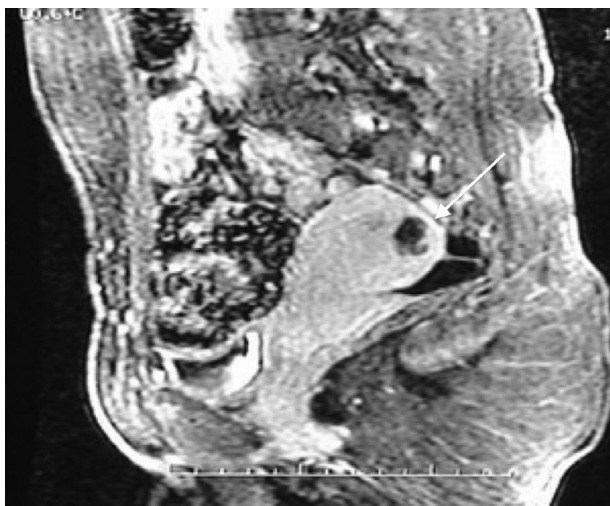


Figure 21 Epithelioid trophoblastic tumor. Sagittal gadolinium-enhanced fat-suppressed T1-weighted image showing a heterogeneous and hypovascularized mass in the myometrium (solid arrow).

Table 1 Anatomical Staging According to FIGO Classification (2000)

| Stage | Description |
|-------|---|
| I | GTN strictly confined to the uterine corpus |
| II | GTN extending to the adnexae or to the vagina but limited to genital structures |
| III | GTN extending to the lungs with or without genital tract involvement |
| IV | All other metastatic sites |

Adapted from Ngan et al, 2018³.

the uterus after GTD, due to tumor invasion or surgical manipulation. AVMs can be present in up to 15% of GTD patients and can be diagnosed upon initial presentation of GTD or months after the completion of the treatment.^{37,56,57}

Ultrasound images of AVMs are characterized by myometrial heterogeneous masses with lacunar anechoic structures, representing blood vessels, that are easily visible with Doppler analysis (Fig. 25a and b). Spectral analysis of these vessels usually

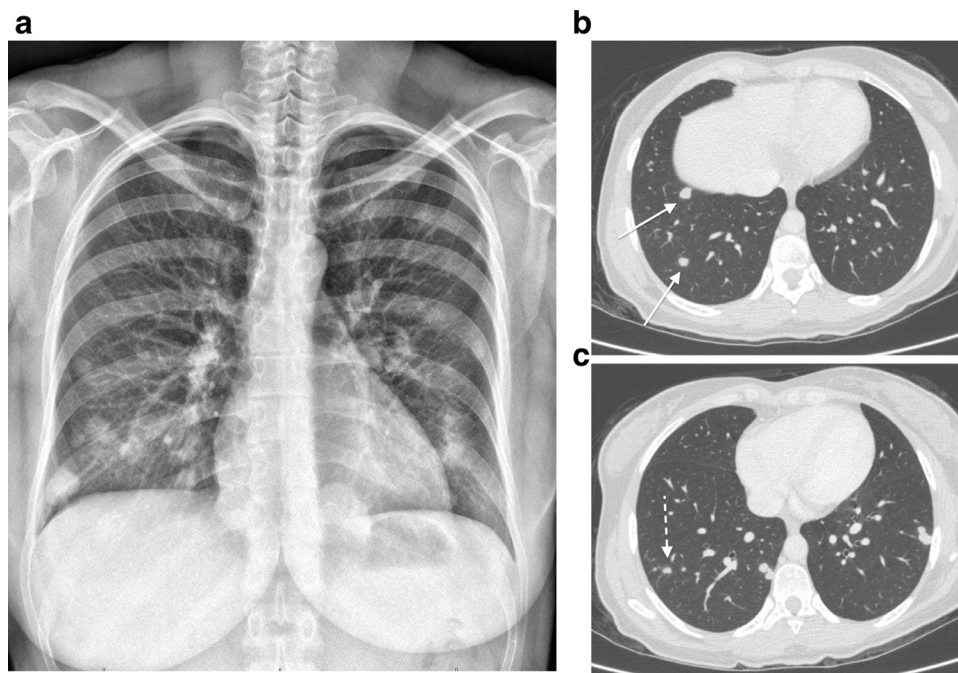


Figure 22 Pulmonary metastases. (a) Anteroposterior CXR showing multiple, round, dense pulmonary nodules. (b) and (c) Axial CT images (lung window) showing multiple bilateral pulmonary nodules (solid arrows). Some nodules are surrounded by ground-glass opacities secondary to peritumoral hemorrhage (dashed arrow).

Table 2 Prognostic Factor Staging System According to FIGO Classification (2000)

| Risk Factor/Score | 0 | 1 | 2 | 4 |
|---|------------------|----------------------------------|----------------------------------|-------------------|
| Age | <40 | >40 | – | – |
| Antecedent pregnancy | Mole | Abortion | Term | – |
| Interval from index pregnancy, months | <4 | 4-6 | 7 a 12 | > 12 |
| Pretreatment hCG level, mIU/mL | <10 ³ | 10 ³ -10 ⁴ | 10 ⁴ -10 ⁵ | > 10 ⁵ |
| Largest tumor size including the uterus, cm | – | 3-4 | ≥ 5 | – |
| Site of metastases | Lung | Spleen, kidney | Gastrointestinal tract | Brain, liver |
| Number of metastases identified | – | 1-4 | 5-8 | > 8 |
| Previous failed chemotherapy | – | – | Single drug | Two or more drugs |

Adapted from Ngan et al, 2018³.

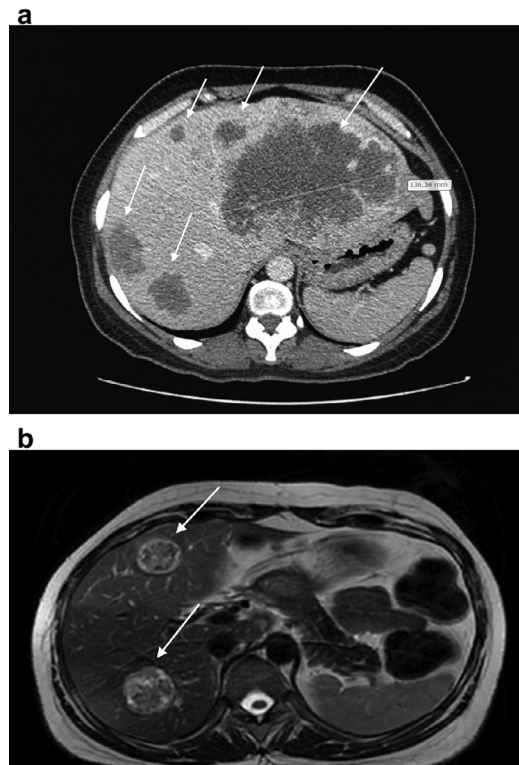


Figure 23 Liver metastases. (a) Axial contrast-enhanced arterial phase CT image showing multiple low-attenuation irregular liver metastases (solid arrows). A CT image of liver metastases was kindly provided by Elza H. Uberti, MD, PhD (Porto Alegre Trophoblastic Disease Center, Porto Alegre, Brazil). (b) Axial T2-weighted image of another patient showing two predominantly hyperintense heterogeneous nodular and rounded liver metastases (solid arrows).

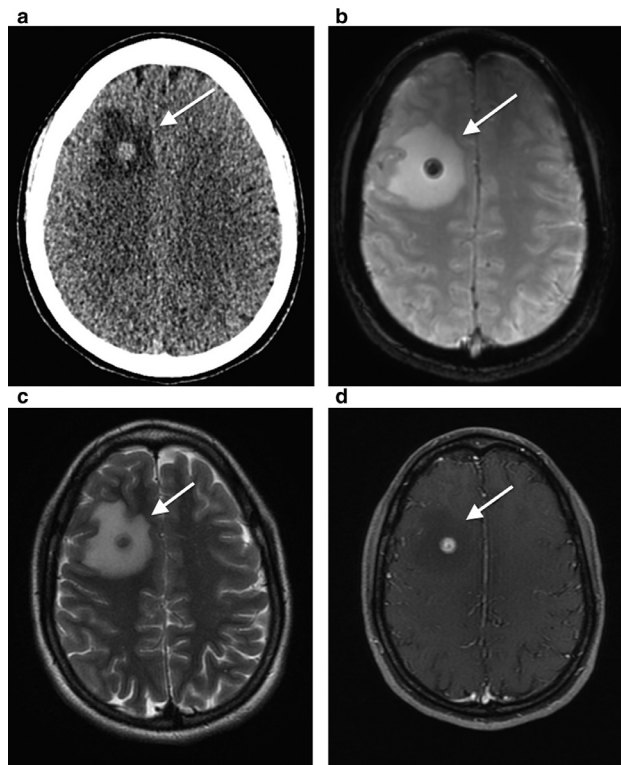


Figure 24 Brain metastasis. (a) Axial nonenhanced CT image showing a right frontal hyperattenuating lesion due to the presence of hemorrhage (solid arrow). (b) Axial susceptibility-weighted imaging (SWI) showing markedly low signal due to blood degradation products (solid arrow). (c) Axial T2-weighted image showing the lesion surrounded by extensive vasogenic edema in the right frontal lobe (solid arrow). (d) Axial gadolinium-enhanced fat-suppressed T1-weighted image showing heterogeneous and intense enhancement of the lesion (solid arrow).

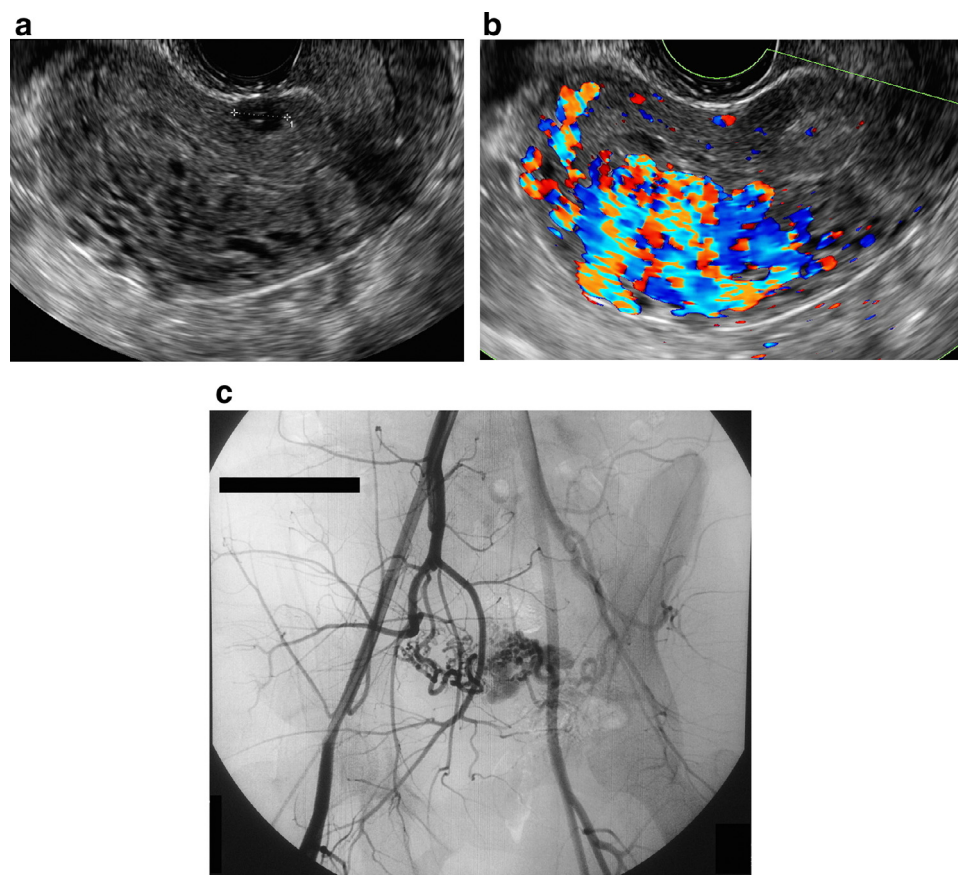


Figure 25 Uterine arteriovenous malformation. (a) Transvaginal grayscale ultrasound image showing a sagittal section of the uterus with a small hypoechogenic nodule in the anterior wall, suggestive of a fibroid, and a large heterogeneous mass in the posterior wall with thin tubular anechoic structures in a patient with undetectable hCG levels during postmolar follow-up. (b) Transvaginal power Doppler ultrasound image showing that the thin tubular anechoic structures within the mass corresponded to various blood vessels with multidirectional turbulent flow. (c) Angiography showing an increased number and caliber of uterine vessels.

reveals low resistance blood flow. AVM is a differential diagnosis for GTN, since the sonographic and Doppler appearances of these lesions are quite similar; therefore, hCG levels are fundamental for distinguishing these 2 entities. MRI can aid in the diagnosis and typically shows a uterine mass with numerous vessels with postgadolinium signal enhancement.^{37,56,57}

Angiographic evaluation of AVMs reveals numerous enlarged uterine vessels with early venous drainage (Fig. 25c). Medical treatment or selective embolization of the uterine arteries can be used as a treatment option for symptomatic AVMs in patients who want to preserve their fertility.^{37,56,57}

Conclusion

GTD is a spectrum of benign and malignant diseases arising from placental trophoblasts. Quantitative measurement of hCG levels plays a central role in the diagnosis and follow-up of GTD, as hCG is a biomarker of this group of diseases; however, imaging is always needed to complement the evaluation

of these patients. Ultrasound is the primary tool for diagnosis of hydatidiform mole. In patients with GTN, imaging modalities are fundamental in the assessment of local and metastatic disease; imaging evaluation usually starts with Doppler ultrasound and CXRs, while CT, MRI, or PET/CT are useful in selected cases. Therefore, radiologists play a key role in the evaluation and management of patients with GTD.

Conflict of Interest

The authors declare that there is no conflict of interest regarding the publication of this article.

Acknowledgment

We would like to thank Elza H. Uberti, MD, Ph.D. (Porto Alegre Trophoblastic Disease Center, Porto Alegre, Brazil) for kindly providing a CT image of hepatic metastases.

References

- Seckl MJ, Sebire NJ, Berkowitz RS: Gestational trophoblastic disease. *Lancet* 376:717-729, 2010
- Lurain JR: Gestational trophoblastic disease I: Epidemiology, pathology, clinical presentation and diagnosis of gestational trophoblastic disease, and management of hydatidiform mole. *Am J Obstet Gynecol* 203:531-539, 2010
- Ngan HYS, Seckl MJ, Berkowitz RS, et al: Update on the diagnosis and management of gestational trophoblastic disease. *Int J Gynaecol Obstet* 143:79-85, 2018
- Cheung ANY: Pathology of gestational trophoblastic diseases. *Best Pract Res Clin Obstet Gynaecol* 17:849-868, 2003
- Lurain JR: Gestational trophoblastic disease II: Classification and management of gestational trophoblastic neoplasia. *Am J Obstet Gynecol* 204:11-18, 2011
- Shaaban AM, Rezvani M, Haroun RR, et al: Gestational trophoblastic disease: Clinical and imaging features. *Radiographics* 37:681-700, 2017
- Lima L, Parente RCM, Maestá I, et al: Clinical and radiological correlations in patients with gestational trophoblastic disease. *Radiol Bras* 49:241-250, 2016
- Steigrad SJ: Epidemiology of gestational trophoblastic diseases. *Best Pract Res Clin Obstet Gynaecol* 17:837-847, 2003
- Fisher RA, Hodges MD: Genomic imprinting in gestational trophoblastic disease—a review. *Placenta* 24 Suppl A:S111-S118, 2003
- Sun SY, Melamed A, Goldstein DP, et al: Changing presentation of complete hydatidiform mole at the New England Trophoblastic Disease Center over the past three decades: Does early diagnosis alter risk for gestational trophoblastic neoplasia? *Gynecol Oncol*. 138:46-49, 2015
- Braga A, Moraes V, Maestá I, et al: Changing trends in the clinical presentation and management of complete hydatidiform mole among Brazilian women. *Int J Gynecol Cancer* 26:984-990, 2016
- Bajaj SK, Misra R, Gupta R, et al: Complete hydatidiform mole with coexisting twin fetus: Usefulness of MRI in management planning. *J Obstet Gynecol India* 64:9-13, 2013
- Imafuku H, Miyahara Y, Ebina Y, et al: Ultrasound and MRI findings of twin pregnancies with complete hydatidiform mole and coexisting normal fetus: Two case reports. *Kobe J Med Sci* 64:E1-E5, 2018
- Cortés-Charry R, Salazar A, García-barrila V, et al: Hydatidiform mole in ectopic pregnancy. Clinical, imaging, pathological and immunohistochemical characteristics. *J Reprod Med* 57:329-332, 2011
- Braga A, Uberti EMH, Fajardo MDC, et al: Epidemiological report on the treatment of patients with gestational trophoblastic disease in 10 Brazilian referral centers: Results after 12 years since International FIGO 2000 Consensus. *J Reprod Med* 59:241-247, 2013
- Huberman RP, Fon GT, Bein ME: Benign molar pregnancies: Pulmonary complications. *Am J Roentgenol* 138:71-74, 1982
- Ball L, Vercesi V, Costantino F, et al: Lung imaging: How to get better look inside the lung. *Ann Transl Med* 5:294, 2017
- Berkowitz RS, Goldstein DP: Clinical practice. Molar pregnancy. *N Engl J Med* 360:1639-1645, 2009
- Fowler DJ, Lindsay I, Seckl MJ, et al: Routine pre-evacuation ultrasound diagnosis of hydatidiform mole: Experience of more than 1000 cases from a regional referral center. *Ultrasound Obstet Gynecol* 27:56-60, 2006
- Jauniaux E, Memtsa M, Johns J, et al: New insights in the pathophysiology of complete hydatidiform mole. *Placenta* 62:28-33, 2018
- Sebire NJ, Rees H, Paradinás F, et al: The diagnostic implications of routine ultrasound examination in histologically confirmed early molar pregnancies. *Ultrasound Obstet Gynecol* 18:662-665, 2001
- Fowler DJ, Lindsay I, Seckl MJ, et al: Histomorphometric features of hydatidiform moles in early pregnancy: Relationship to detectability by ultrasound examination. *Ultrasound Obstet Gynecol* 29:76-80, 2007
- Romero R, Horgan JG, Kohorn EI, et al: New criteria for the diagnosis of gestational trophoblastic disease. *Obstet Gynecol* 66:553-558, 1985
- Jauniaux E: Ultrasound diagnosis and follow-up of gestational trophoblastic disease. *Ultrasound Obstet Gynecol* 11:367-377, 1998
- Fine C, Bundy A, Berkowitz R, et al: Sonographic diagnosis of partial hydatidiform mole. *Obstet Gynecol* 73:414-418, 1989
- Scholz NB, Bolund L, Nyegaard M, et al: Triploidy—observations in 154 diandric cases. *PLoS One* 10:e0142545, 2015
- Lin LH, Maestá I, Braga A, et al: Multiple pregnancies with complete mole and coexisting normal fetus in North and South America: A retrospective multicenter cohort and literature review. *Gynecol Oncol* 145:88-95, 2017
- Sebire NJ, Foskett M, Paradinás FJ, et al: Outcome of twin pregnancies with complete hydatidiform mole and healthy co-twin. *Lancet* 359:2165-2166, 2002
- Hassadia A, Kew F, Tidy J, et al: Ectopic gestational trophoblastic disease. A case series review. *J Reprod Med*. 57:297-300, 2011
- Muto MG, Lage JM, Berkowitz RS, et al: Gestational trophoblastic disease of the fallopian tube. *J Reprod Med* 36:57-60, 1991
- Lu D, Tang JJ, Zakashansky K, et al: Heterotopic pregnancy including intrauterine normal gestation and tubal complete hydatidiform mole: A case report and review of the literature. *Int J Gynecol Pathol* 36:428-432, 2017
- Lin LH, Fushida K, Hase EA, et al: Gestational tubal choriocarcinoma presenting as a pregnancy of unknown location following ovarian induction. *Case Rep Obstet Gynecol* 2018:1-6, 2018
- Yamada Y, Ohira S, Yamazaki T, et al: Ectopic molar pregnancy: Diagnostic efficacy of magnetic resonance imaging and review of the literature. *Case Rep Obstet Gynecol* 2016:1-7, 2016
- Hanna RK, Soper JT: The role of surgery and radiation therapy in the management of gestational trophoblastic disease. *Oncologist* 15:593-600, 2010
- Kohorn EI: Clinical management and neoplastic sequelae of trophoblastic embolization associated with hydatidiform mole. *Obstet Gynecol Surv* 42:484-488, 1987
- Tidy JA, Gillespie AM, Bright N, et al: Gestational trophoblastic disease: A study of mode of evacuation and subsequent need for treatment with chemotherapy. *Gynecol Oncol* 78:309-312, 2000
- Braga A, Lima L, Parente RCM, et al: Management of symptomatic uterine arteriovenous malformations after gestational trophoblastic disease: The Brazilian experience and possible role for depot medroxyprogesterone acetate and tranexamic acid treatment. *J Reprod Med* 63:228-239, 2018
- Zhou Q, Lei XY, Xie Q, et al: Sonographic and Doppler imaging in the diagnosis and treatment of gestational trophoblastic disease: A 12-year experience. *J Ultrasound Med* 24:15-24, 2005
- Lin LH, Bernardes LS, Hase EA, et al: Is Doppler ultrasound useful for evaluating gestational trophoblastic disease? *Clinics* 70:810-815, 2015
- Lin LH, Fushida K, Okumura M, et al: Single-center experience in managing epithelioid trophoblastic tumors. *J Reprod Med* 63:271-275, 2018
- Horowitz NS, Goldstein DP, Berkowitz RS: Placental site trophoblastic tumors and epithelioid trophoblastic tumors: Biology, natural history, and treatment modalities. *Gynecol Oncol* 144:208-214, 2016
- Hsieh F, Lee C, Chen T: Vascular patterns of gestational trophoblastic tumors by color Doppler ultrasound. *Cancer* 74:2361-2365, 1994
- Sita-Lumsden A, Medani H, Fisher R, et al: Uterine artery pulsatility index improves prediction of methotrexate resistance in women with gestational trophoblastic neoplasia with FIGO score 5-6. *BJOG* 120:1012-1015, 2013
- Agarwal R, Harding V, Short D, et al: Uterine artery pulsatility index: A predictor of methotrexate resistance in gestational trophoblastic neoplasia. *Br J Cancer* 106:1089-1094, 2012
- Asmar FTC, Braga-Neto AR, Rezende-Filho J, et al: Uterine artery Doppler flow velocimetry parameters for predicting gestational trophoblastic neoplasia after complete hydatidiform mole, a prospective cohort study. *Clinics* 72:284-288, 2017
- Dhanda S, Ramani S, Thakur M: Gestational trophoblastic disease: A multimodality imaging approach with impact on diagnosis and management. *Radiol Res Pract* 2014:1-12, 2014
- Seckl MJ, Sebire NJ, Fisher RA, et al: Gestational trophoblastic disease: ESMO clinical practice guidelines for diagnosis, treatment and follow-up. *Ann Oncol* 24:vi39-vi50, 2013
- Darby S, Jolley I, Pennington S, et al: Does chest CT matter in the staging of GTN? *Gynecol Oncol* 112:155-160, 2009
- Price JM, Lo C, Abdi S, et al: The role of computed tomography scanning of the thorax in the initial assessment of gestational trophoblastic neoplasia. *Int J Gynecol Cancer* 25:1731-1736, 2015

50. McGrath S, Short D, Harvey R, et al: The management and outcome of women with post-hydatidiform mole "low-risk" gestational trophoblastic neoplasia, but hCG levels in excess of 100 000 IU l⁻¹. *Br J Cancer* 102:810-814, 2010
51. Diver E, May T, Vargas R, et al: Changes in clinical presentation of post-term choriocarcinoma at the New England Trophoblastic Disease Center in recent years. *Gynecol Oncol* 130:483-486, 2013
52. Li J, Yang J, Liu P, et al: Clinical characteristics and prognosis of 272 postterm choriocarcinoma patients at Peking Union Medical College Hospital: A retrospective cohort study. *BMC Cancer* 16:1-8, 2016
53. Xiao C, Yang J, Zhao J, et al: Management and prognosis of patients with brain metastasis from gestational trophoblastic neoplasia: A 24-year experience in Peking union medical college hospital. *BMC Cancer* 15:1-10, 2015
54. Agarwal R, Alifrangis C, Everard J, et al: Management and survival of patients with FIGO high-risk gestational trophoblastic Neoplasia: The U.K. Experience, 1995-2010. *J Reprod Med* 59:7-12, 2014
55. Mangili G, Bergamini A, Giorgione V, et al: [18F]fluorodeoxyglucose positron emission tomography/computed tomography and trophoblastic disease: The gynecologist perspective. *Q J Nucl Med Mol Imaging* 60:103-116, 2016. 2016;60(2):103-16
56. Lim AKP, Agarwal R, Seckl MJ, et al: Embolization of bleeding residual uterine vascular malformations in patients with treated gestational trophoblastic tumors. *Radiology* 222:640-644, 2002
57. Touhami O, Gregoire J, Noel P, et al: Uterine arteriovenous malformations following gestational trophoblastic neoplasia: A systematic review. *Eur J Obstet Gynecol Reprod Biol* 181:54-59, 2014